Deciphering the Contributions of Volcanic and Environmental Events to Temporal Velocity Variations in Kamchatka (Russia)

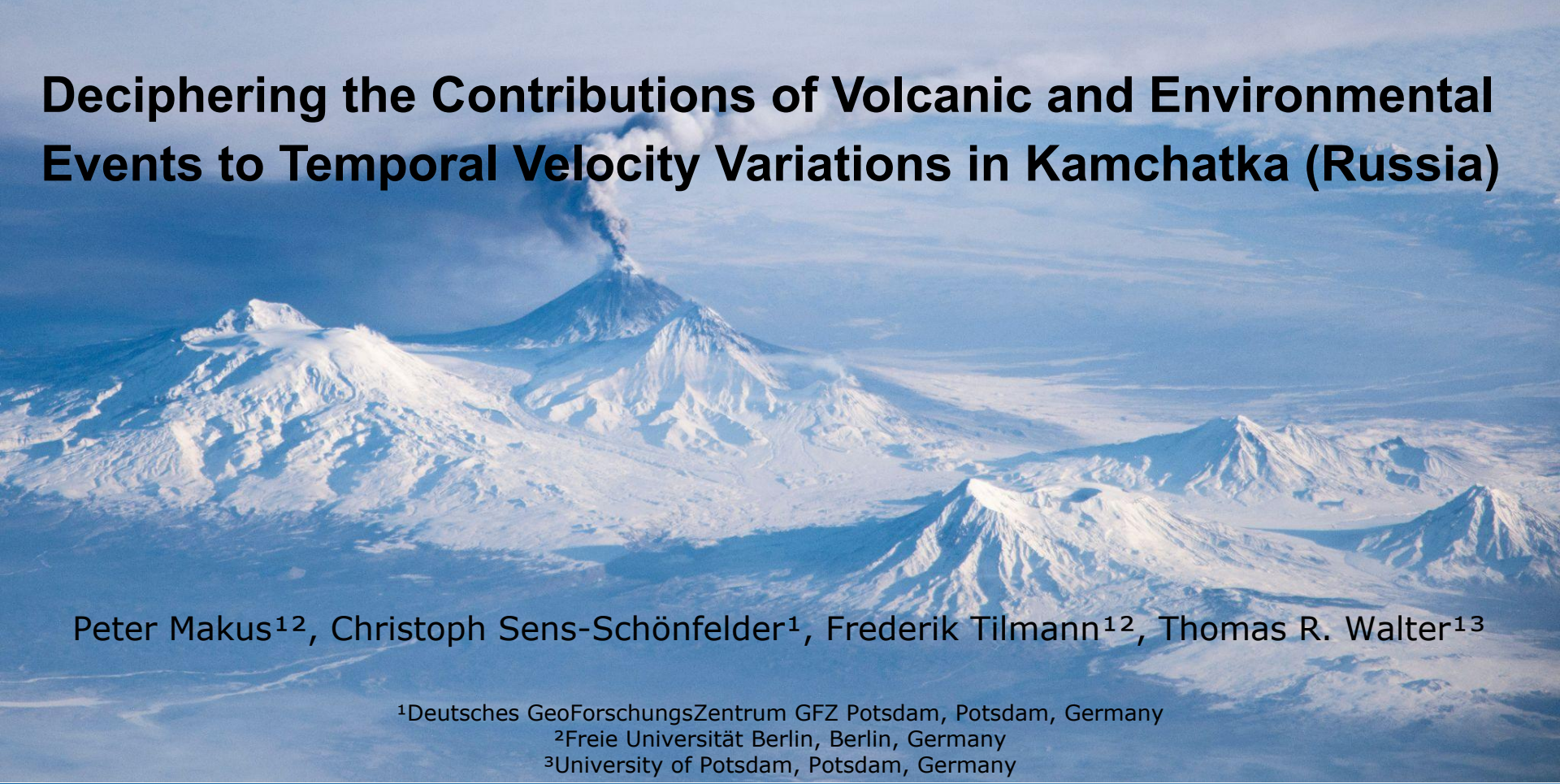

Peter Makus[1,2], Christoph Sens-Schönfelder[1], Frederik Tilmann[1,2], Thomas R. Walter[1,3]

[1]Deutsches GeoForschungsZentrum GFZ Potsdam, Potsdam, Germany
[2]Freie Universität Berlin, Berlin, Germany
[3]University of Potsdam, Potsdam, Germany

GFZ Helmholtz Centre Potsdam

HELMHOLTZ

Motivation: Improving the Reliability of Eruption Forecasts

For decades, if not centuries, scientists have been looking for methods to improve the accuracy and reliability of volcano eruption forecasts. They have done so utilising a multitude of techniques from different disciplines. Recently, some studies have detected increases in seismic velocity related to volcanic inflation events (e.g., Donaldson et al., 2017; Hirose et al. 2017; Obermann et al., 2013). We adopt seismological passive monitoring techniques to examine the temporal variability of the regional velocity structure at the Klyuchevskoy Volcano Group (KVG) in Kamchatka, Russia.

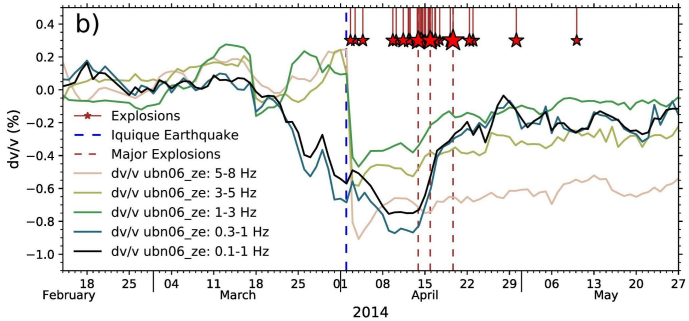

Machacca-Puma, et al., 2019

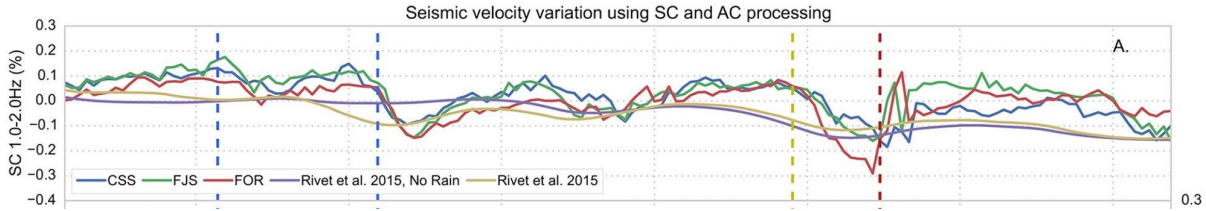

De Plaen, et al., 2016

Overview

- Theory

  Introduction to monitoring with ambient seismic noise
- Data, Processing, and Clustering of Noise Correlations

  Provides an overview over the available data, the applied processing, and introduces a new noise interferometry software. Also, discusses the methods we used to find time windows that yield stable dv/v estimates.
- Spatial Stacking

  Describes the procedure we use and groups we find to stack interferometric results from several stations.
- Results and Discussion

  Shows the resulting velocity times series for three groups of stations. We find responses to seismic events, environmental factors, and indicators for the beginning of an inflation at Bezymianny volcano.

Click on the coloured text to follow hyperlinks to different sections of the material. You can always click on the small volcano at the bottom to return to this slide.

Theory

Retrieving dv/v from Ambient Noise

Seismic ambient noise is the ubiquitous, ocean-generated background chatter of the subsurface. It can be shown that the correlation of recordings of this field equals the Green's function of the medium between the recording points (or detectors, see figure) if the noise field is homogeneous and uniform in space, time, and frequency (for a detailed discussion of the theory see, e.g., Nakata, et al., 2019**).**

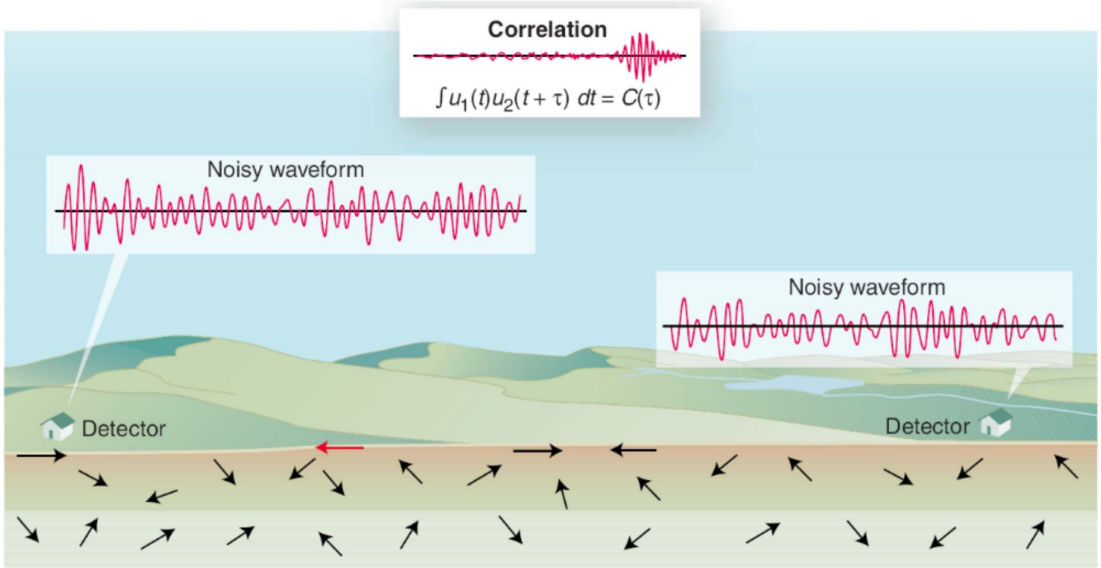

(courtesy of ISTerre, Grenoble)

Retrieving dv/v from Ambient Noise

We can examine the change of the noise correlations (or Green's function estimates) to quantify the evolution of the medium's seismic velocity in the medium. Here, we use the trace stretching technique (Sens-Schönfelder, et al., 2006). The algorithm first extracts a representative reference correlation function that is then iteratively correlated with each correlation stretched by a set of stretch values. The highest correlating stretch is assumed to be proportional to a homogeneous velocity change -dv/v.

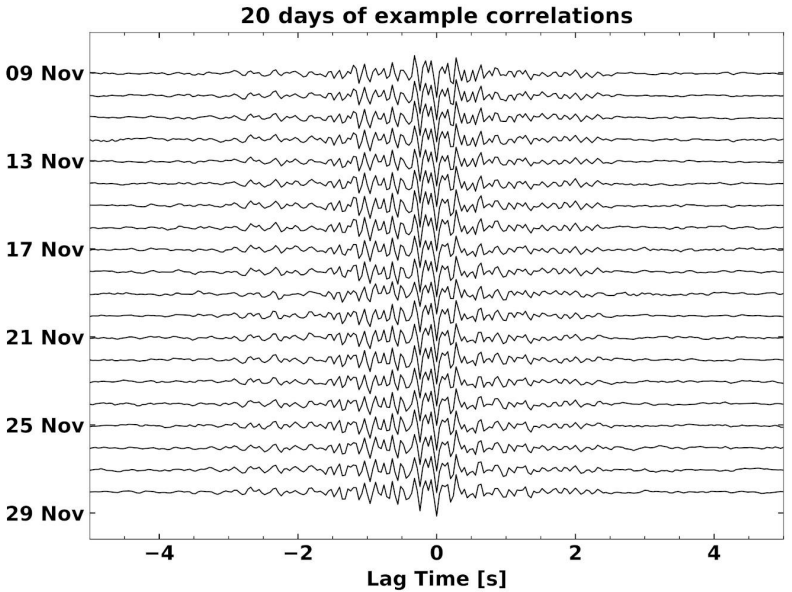

Fig: Daily Correlations show minute changes of the velocity structure.

Data, Processing, and Clustering of Noise Correlations

Region & Data

- Kamchatka is home to the Klyuchevskoy Volcano Group (KVG) - one of the most active subduction zone volcano clusters world-wide
- 1 year of continuous waveform data: summer 2015 to summer 2016
- Recordings from 101 seismic stations are available, belonging to the permanent Kamchatka network and the temporary KISS deployment (Shapiro et al., 2017)

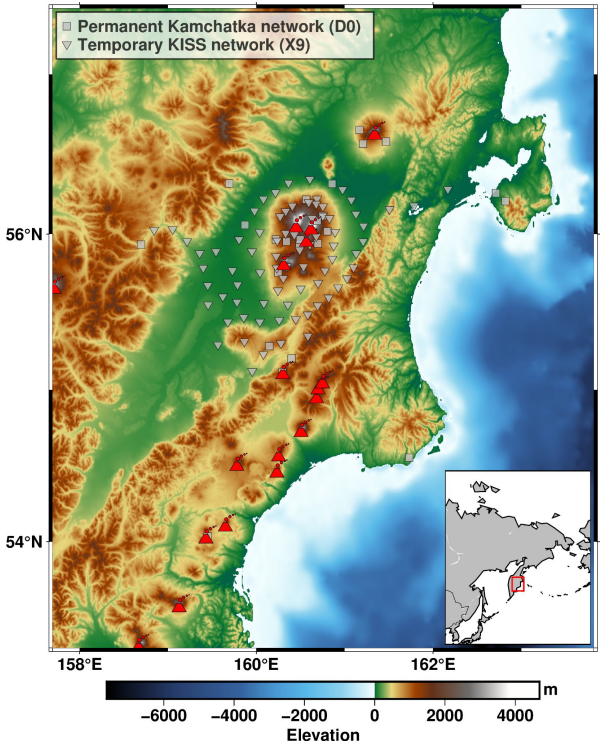

Fig: Distribution of the seismic stations on Kamchatka. Squares represent permanent stations, whereas inverted triangles are part of the temporary KISS deployment. The locations of active volcanic centres are depicted.

Processing

We process our data using ***SeisMIC*** - an open-source ambient noise interferometry software available on GitHUB (https://github.com/PeterMakus/SeisMIC). In detail, the processing steps are:

1. Preprocessing: detrending, tapering, bandpass filtering in octave steps, 1-bit normalisation, and spectral whitening (for cross- and auto correlations)
2. Computing auto-, cross- and self-correlations in the Fourier domain
3. Extracting a representative reference correlation.
4. Stretching the time domain of the reference and, for each 1h time window, finding the stretch that yields the highest correlation coefficient. The stretch corresponds to -dv/v.

Kamchatka: A Fluctuating Noise Field

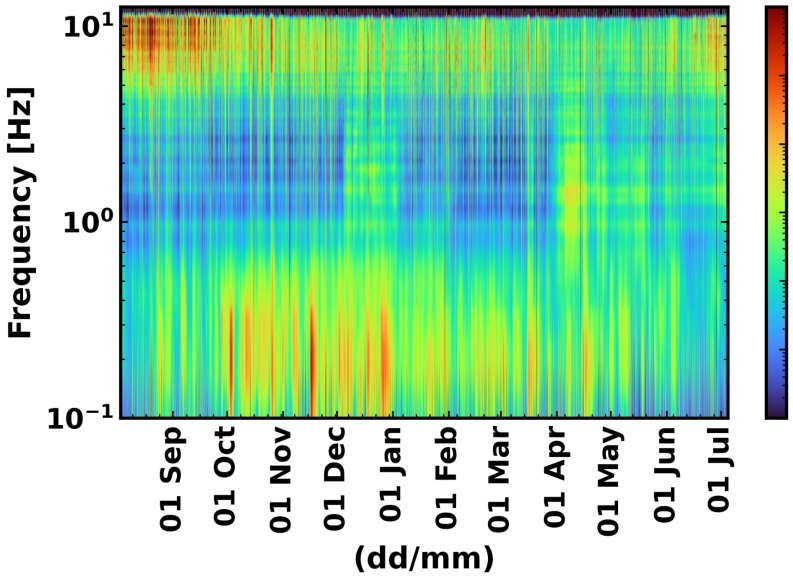

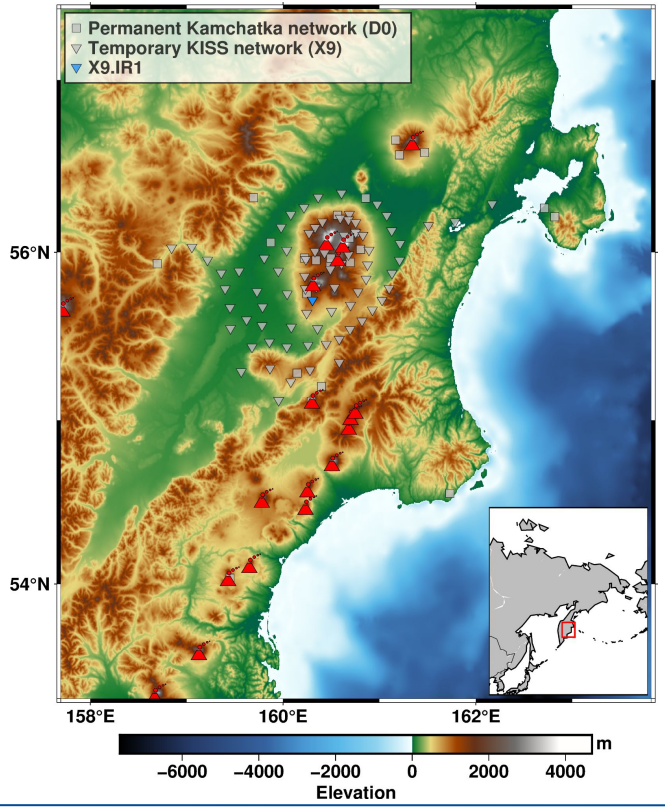

(Left) Power spectrum of the temporary station, X9.IR1, from August 2015 to July 2016 (note, the colour scale is logarithmic). (Right) The location of X9.IR1 is plotted as a blue inverted triangle.

Kamchatka: A Fluctuating Noise Field

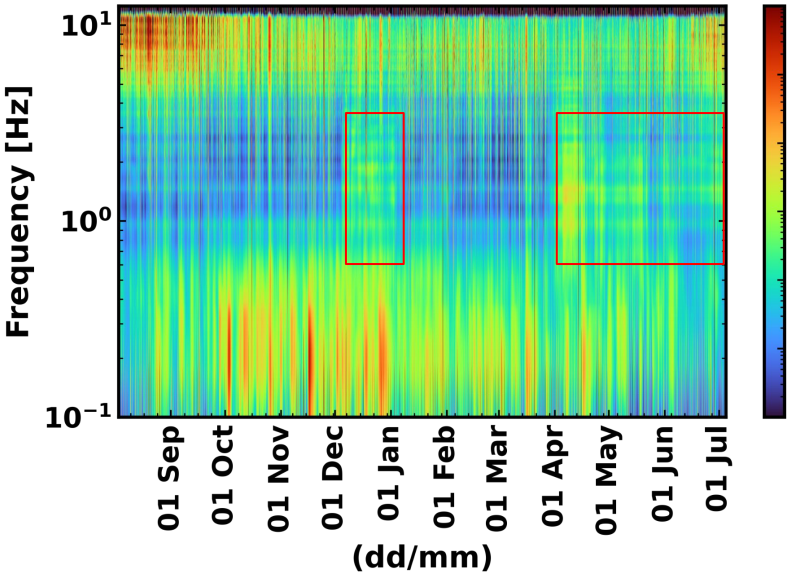

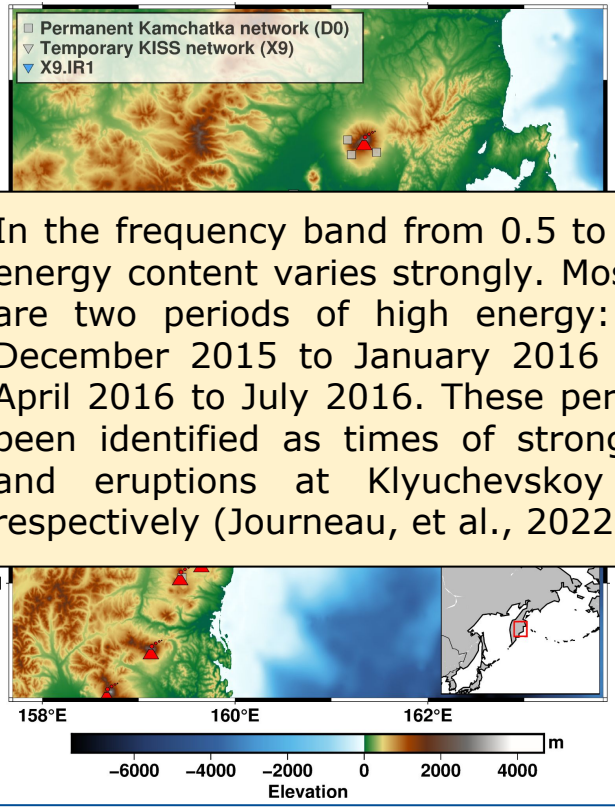

In the frequency band from 0.5 to 5 Hz, the energy content varies strongly. Most notable are two periods of high energy: 1. From December 2015 to January 2016 and from April 2016 to July 2016. These periods have been identified as times of strong tremors and eruptions at Klyuchevskoy volcano, respectively (Journeau, et al., 2022).

(Left) Power spectrum of the temporary station, X9.IR1, from August 2015 to July 2016 (note, the colour scale is logarithmic). (Right) The location of X9.IR1 is plotted as a blue inverted triangle.

uctuating Noise Field

Computing correlations using the preprocessed data from this station results several independent Green's function estimates. Due to their differing shape, these correlations are ill-suited to be compared to each other and the assumptions for the trace stretching method (and other interferometric methods) are broken.

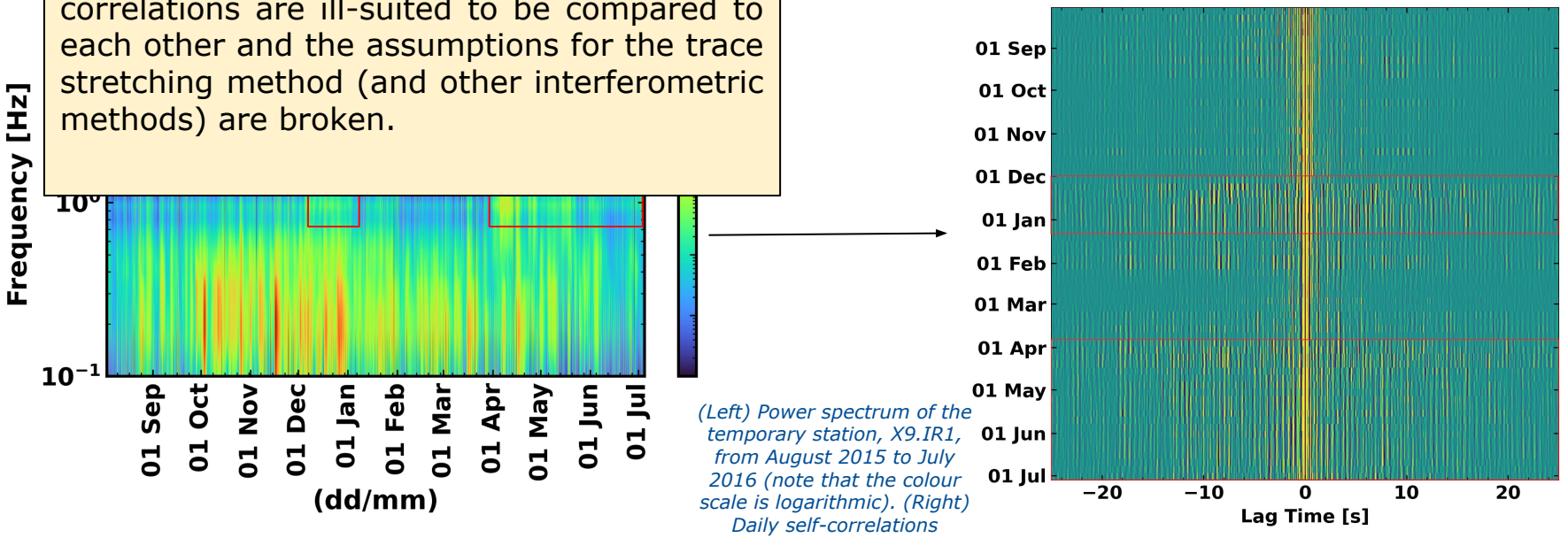

(Left) Power spectrum of the temporary station, X9.IR1, from August 2015 to July 2016 (note that the colour scale is logarithmic). (Right) Daily self-correlations between the E and N component of the processed raw data.

Solution: Separate Monitoring for Similar Green's Function Estimates

We can circumvent this issue by clustering the correlations into groups whose members are close enough to be compared. To these ends, we use a hierarchical clustering algorithm.

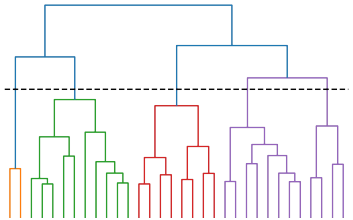

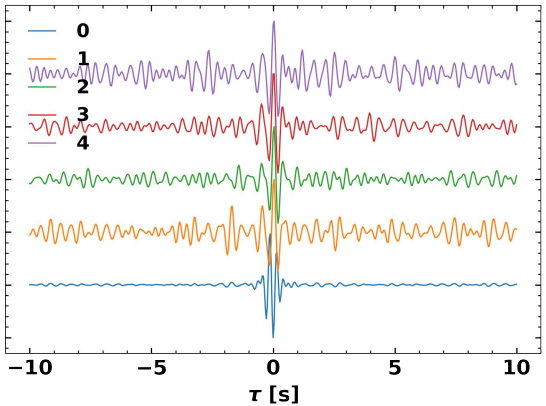

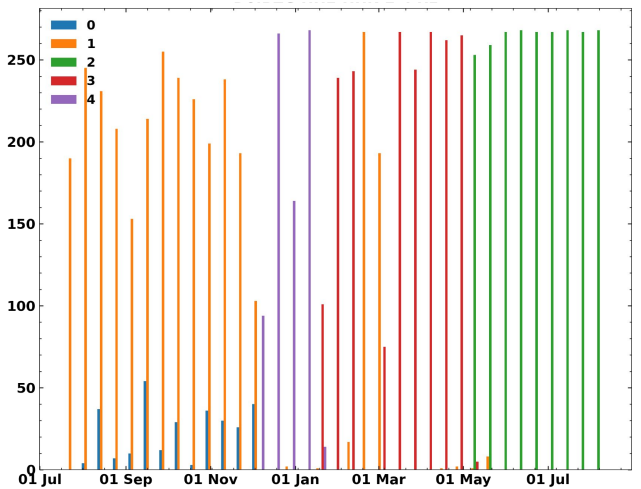

Solution: Separate Monitoring for Similar Green's Function Estimates

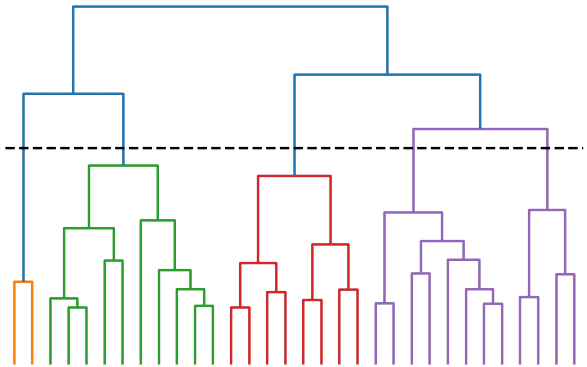

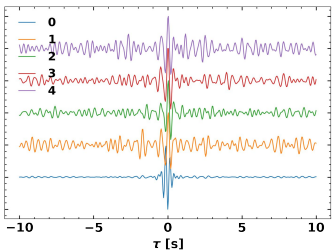

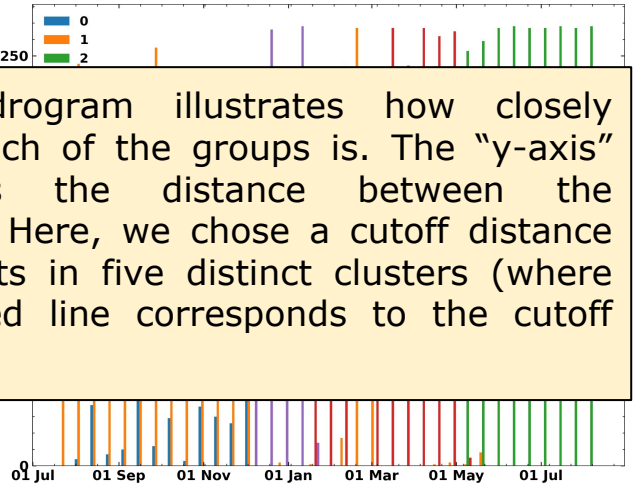

The dendrogram illustrates how closely related each of the groups is. The "y-axis" represents the distance between the branches. Here, we chose a cutoff distance that results in five distinct clusters (where the dashed line corresponds to the cutoff distance).

Solution: Separate Monitoring for Similar Green's Function Estimates

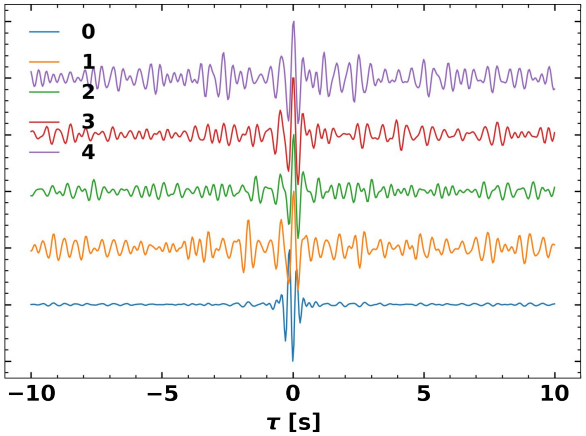

When plotting the average of each cluster, it becomes obvious that the Green's function estimates differ markedly. Only very few phases can be tracked through several groups.

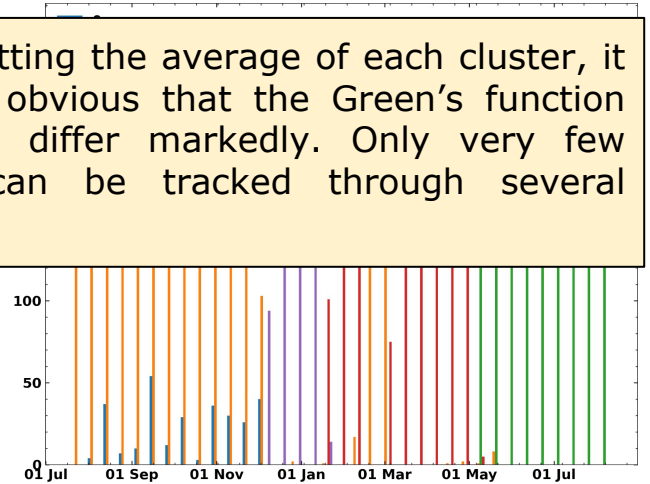

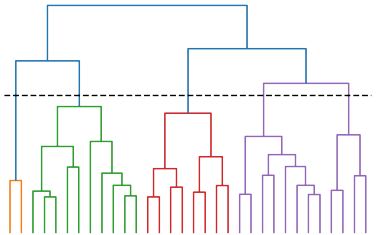

Solution: Separate Monitoring for Similar Green's Function Estimates

The clusters occur temporally close to each other, which points to a short-term stability of the noise field.

Upon closer inspection, we can see that the clusters correspond to different states of volcanic activity reported by Journeau, et al. (2022).

After examining the cluster distribution, we opt to monitor several time periods separately. However, we include all correlations in these times to avoid introducing biases from the clustering.

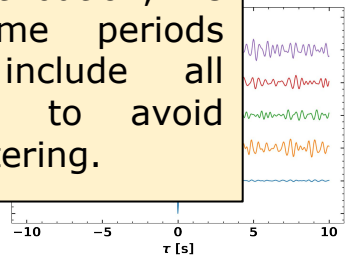

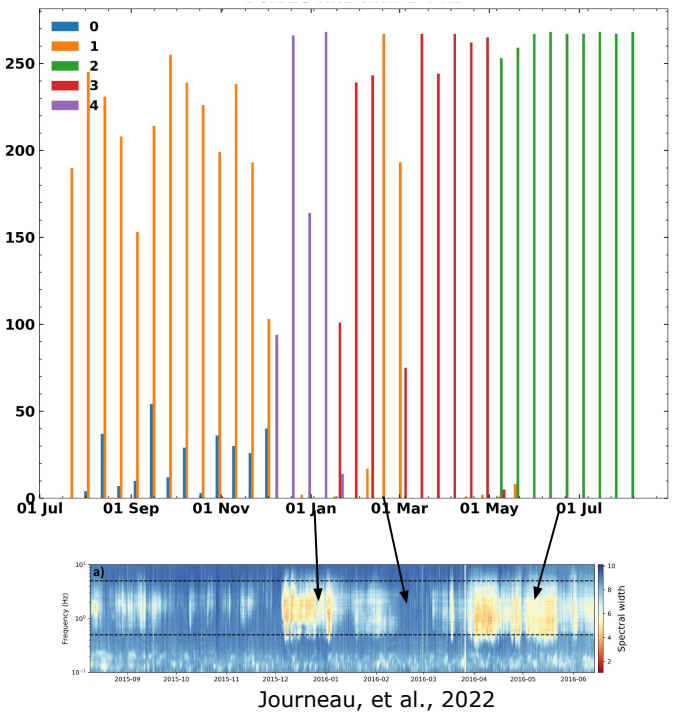

Journeau, et al., 2022

Spatial Stacking

Spatial Stacking

Even when using the selected time windows, dv/v estimates from single combination correlations are rarely stable. To improve stability and temporal resolution, we stack the similarity matrices (i.e., the matrix relating the stretch, time, and correlation coefficient) from several stations. We decide about the stack groups by employing an approach that combines AI-driven analysis (Baron, et al., 2021) and visual inspection of the similarity of the dv/v responses.

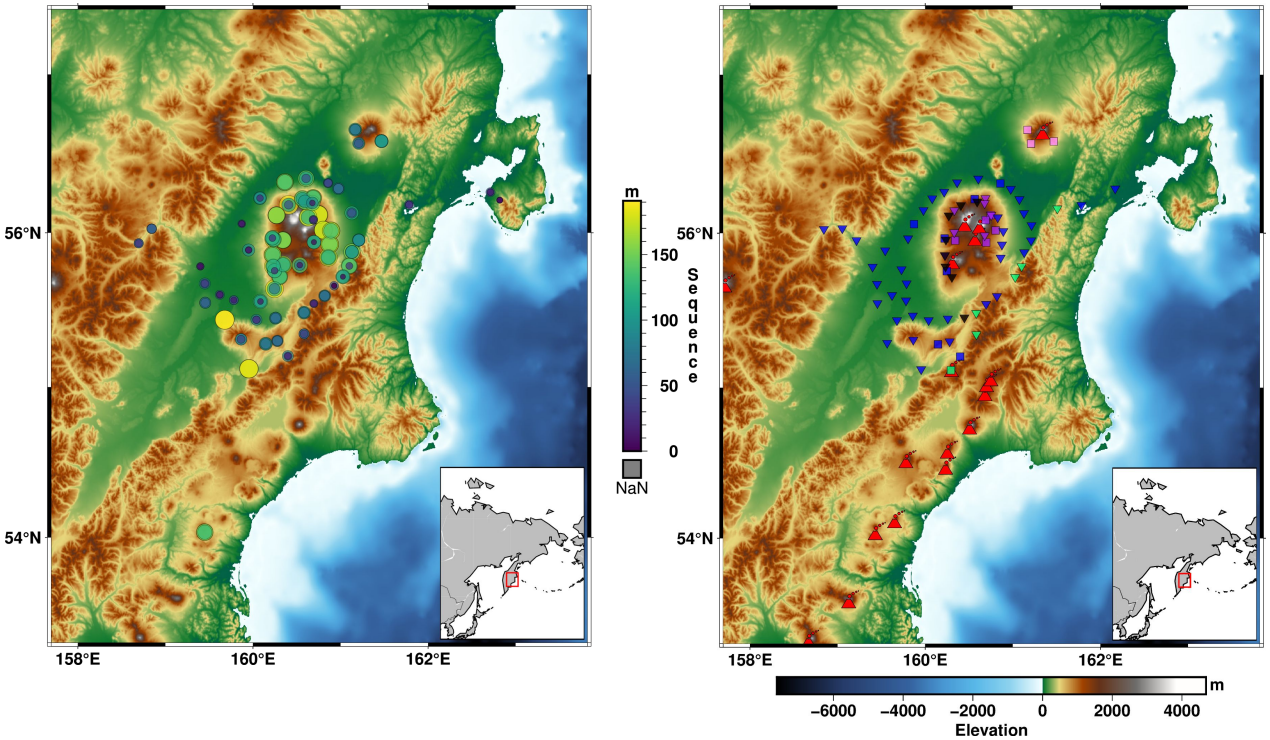

Fig: (Left) Similarity matrices compared using TheSequencer (Baron, et al., 2021). Similarly sized and coloured circles have more similar response. (Right) The final stacking groups.

Spatial Stacking

Fig: (Left) Similarity matrices compared using TheSequencer (Baron, et al., 2021). Similarly sized and coloured circles have more similar response. (Right) The final stacking groups.

The dv/v time series are mainly dependent on geological setting (i.e., stations situated on the ridge in the east, stations in the local sedimentary basin, the Central Kamchatka Depression, and stations that were deployed on the volcanic edifices) and on the station elevation - most likely due to varying seasonal responses.

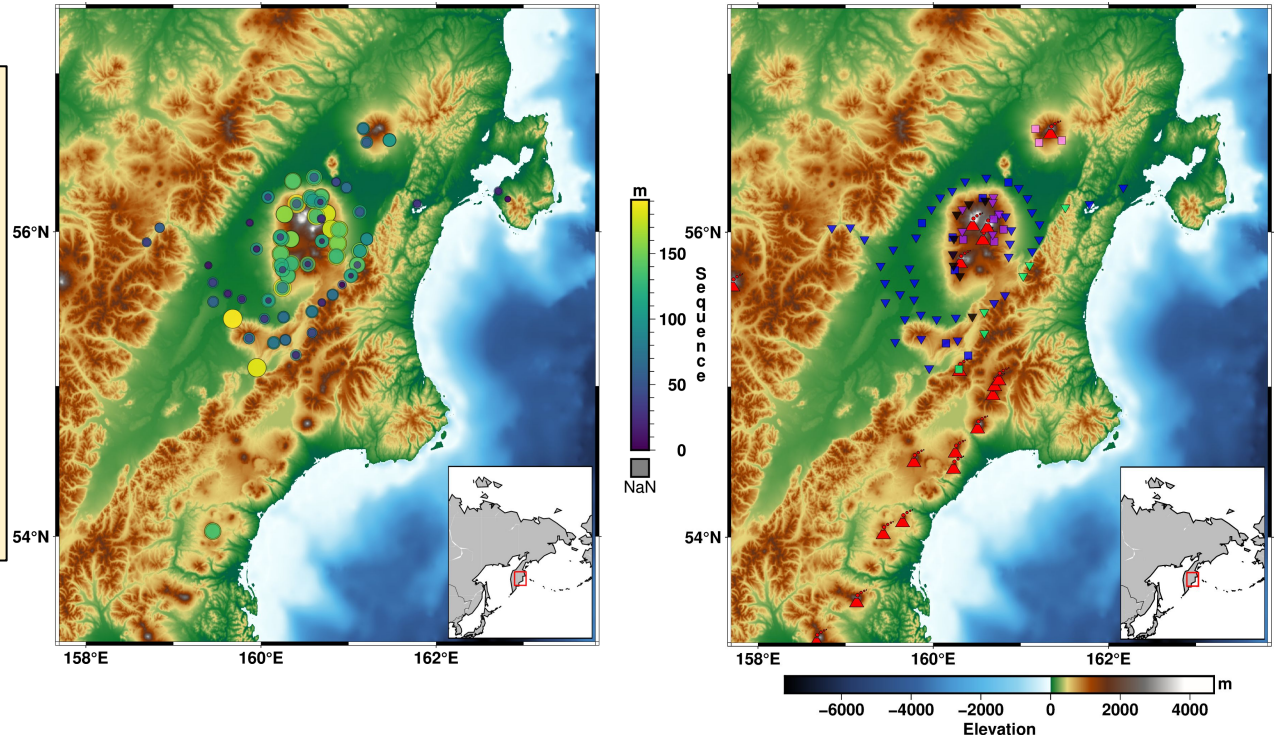

Results & Discussion

Results

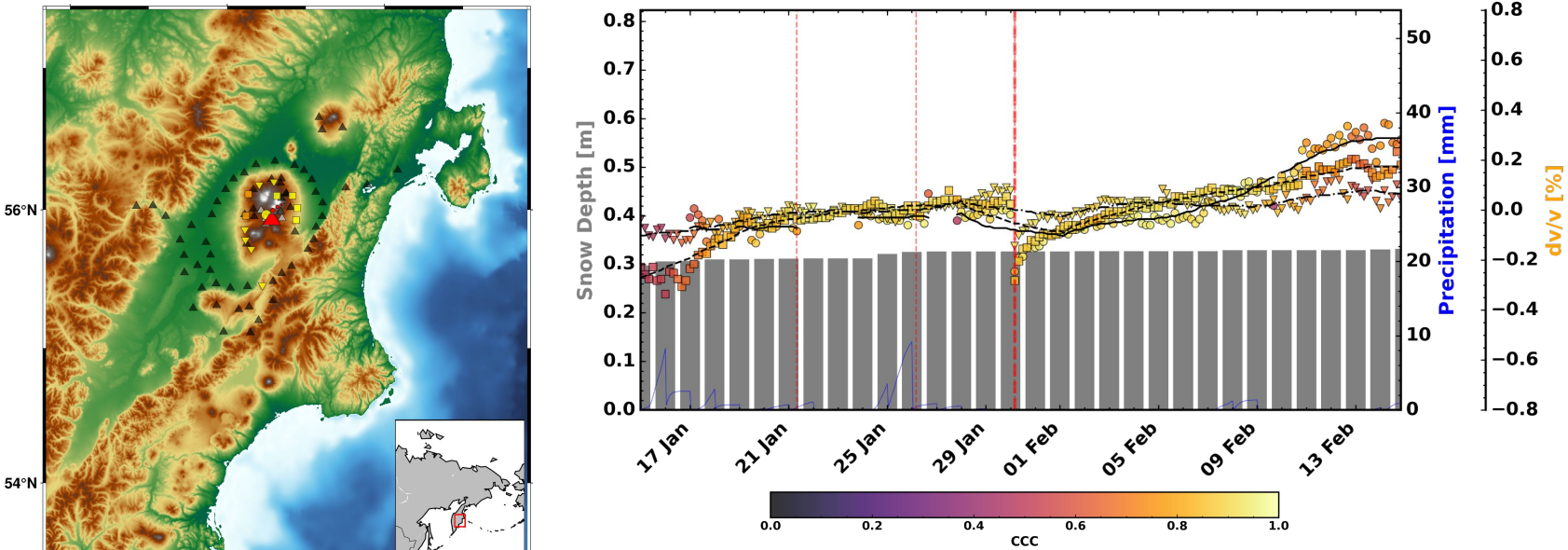

Fig: (Left) A map view of the study area. The location of Bezymianny volcano is depicted.Grey stations are failing or out-of-order during the targeted times. Stations shown in black are available though not discussed. Orange stations are used for the "triangle" and the "square" group. (Right) dv/v time series for coloured groups of stations on the map (symbols are identical). Each point corresponds to the dv/v of a two-hours time window. The points' colour scales with the cumulative correlation coefficient (CCC), i.e., the maximum of the stacked similarity matrix. The dv/v estimated from the two-day smoothed similarity matrices are plotted in black. The blue curve indicates hourly precipitation in water equivalent. Grey bars correspond to the snow-depth in water equivalent. Vertical red-dashed lines are the origin times of local earthquakes with magnitudes>4.8.

Results

The most striking feature in the dv/v curve is a sudden velocity drop across the whole network on January 30th followed by a short period of recovery. We interpret this drop to be caused by a local magnitude 7.2 earthquake striking approximately 100 km south of the networks.

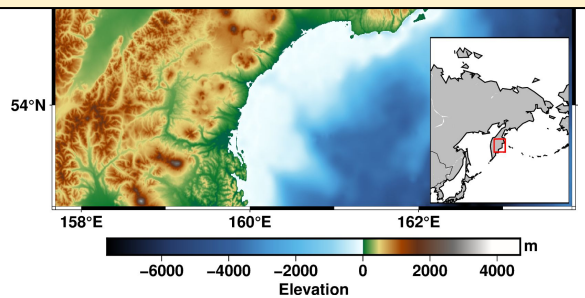

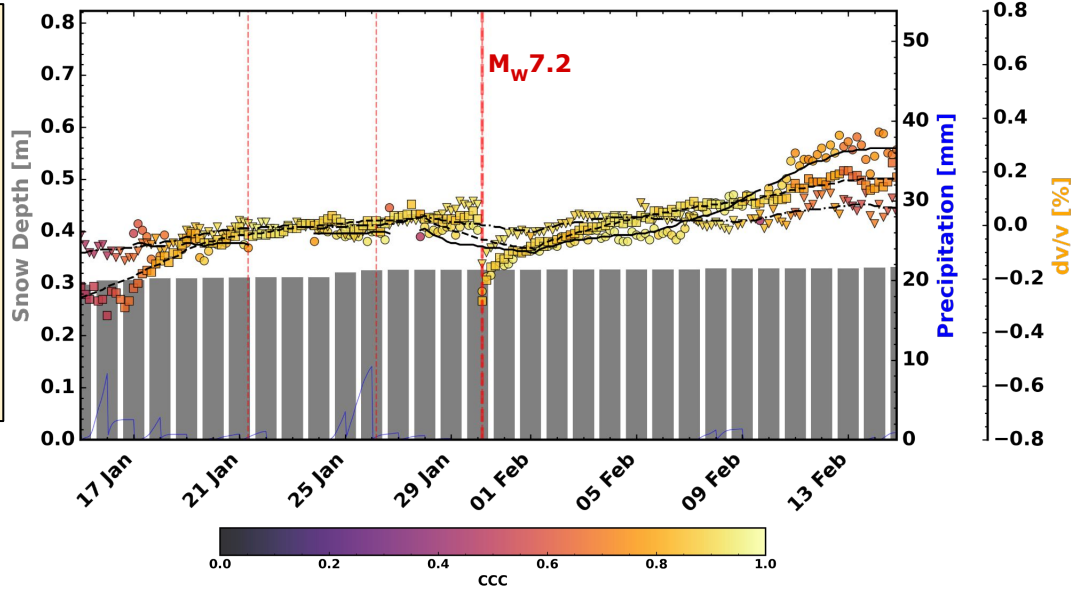

Fig: (Left) A map view of the study area. The location of Bezymianny volcano is depicted.Grey stations are failing or out-of-order during the targeted times. Stations shown in black are available though not discussed. Orange stations are used for the "triangle" and the "square" group. (Right) dv/v time series for coloured groups of stations on the map (symbols are identical). Each point corresponds to the dv/v of a two-hours time window. The points' colour scales with the cumulative correlation coefficient (CCC), i.e., the maximum of the stacked similarity matrix. The dv/v estimated from the two-day smoothed similarity matrices are plotted in black. The blue curve indicates hourly precipitation in water equivalent. Grey bars correspond to the snow-depth in water equivalent. Vertical red-dashed lines are the origin times of local earthquakes with magnitudes>4.8.

Ground Response to the Mw 7.2 30/01/16

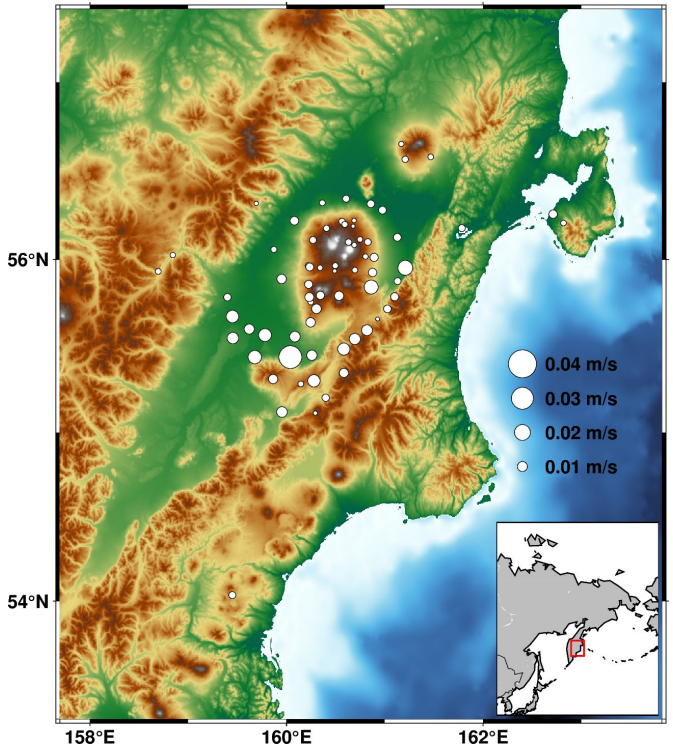

We can compute the peak ground velocities (PGVs). As expected the PGVs are highest for stations closer to the epicentre and in the sedimentary basin.

Fig: The peak ground velocities (PGVs) associated to the magnitude 30/01/16 7.2 event recorded at each of the stations. The circles' radii scale with the PGV. We compute the PGV by picking the maximum of the mean of the envelopes of the horizontal components for each station.

Ground Response to the Mw 7.2 30/01/16

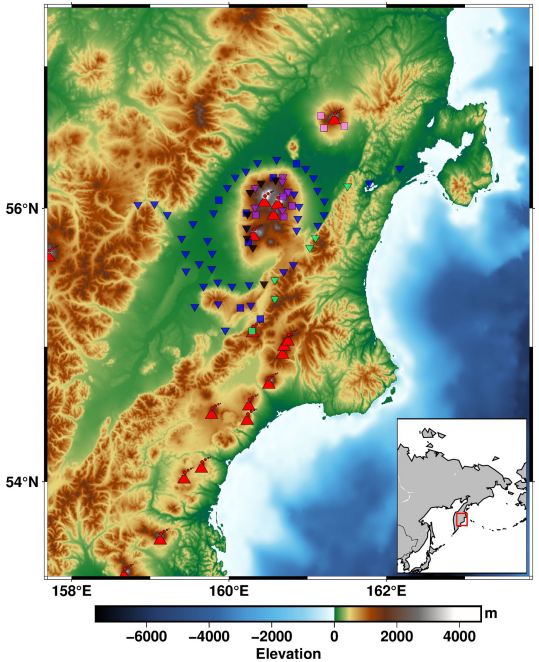

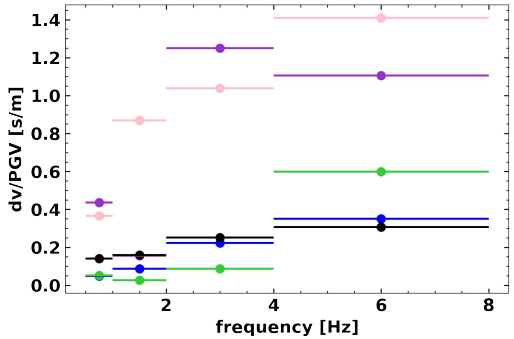

However, the velocity change to PGV ratio shows that volcanic regions have by far the strongest reaction to ground motion. This has already been discussed by Lesage et al. (2014).

Fig: (Left) map of the four stacking groups as discussed in "Spatial Stacking". (Right) (dv/v)/PGV ratios for each of the groups. The colours correspond to the colours used for the different groups in the map. The dv/v drop is the difference between the means of the four dv/v values before and after the event's origin time, respectively.

Results

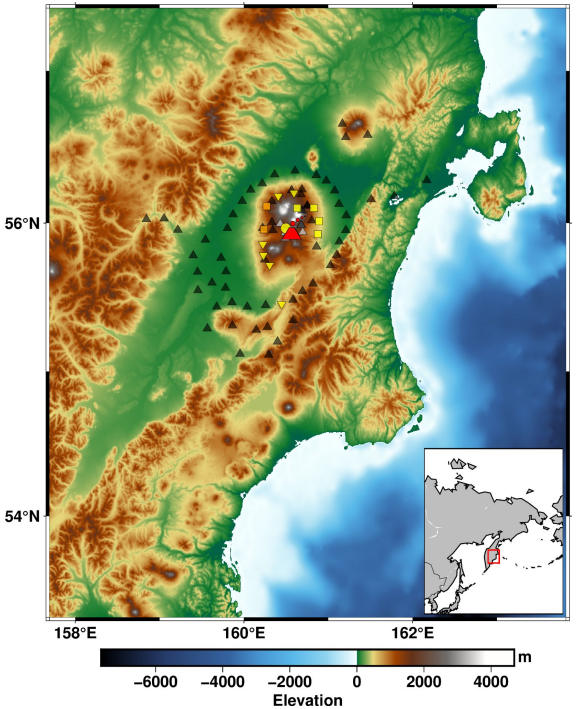

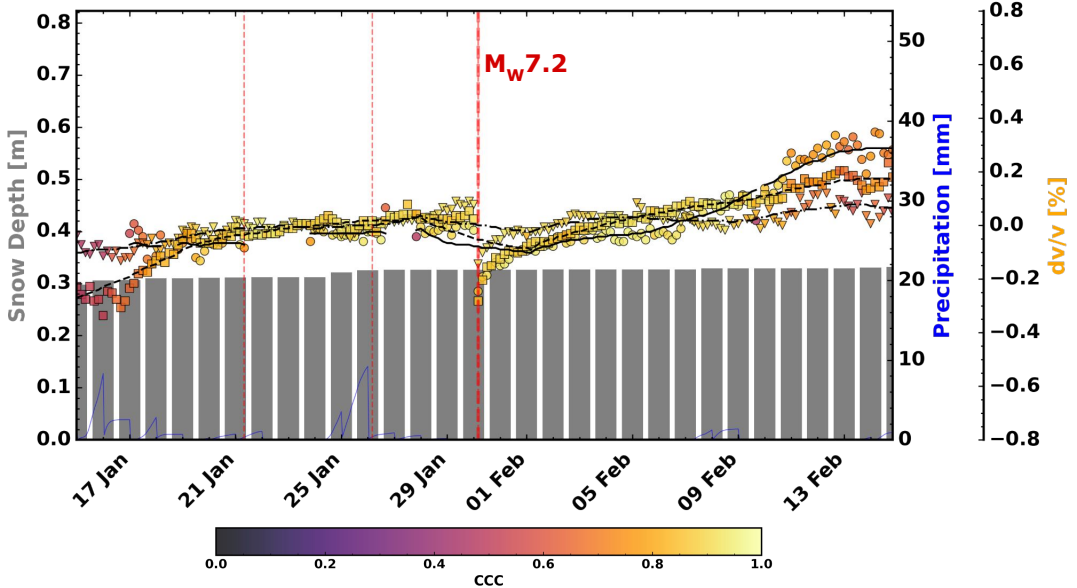

Fig: (Left) A map view of the study area. The location of Bezymianny volcano is depicted.Grey stations are failing or out-of-order during the targeted times. Stations shown in black are available though not discussed. Orange stations are used for the "triangle" and the "square" group. (Right) dv/v time series for coloured groups of stations on the map (symbols are identical). Each point corresponds to the dv/v of a two-hours time window. The points' colour scales with the cumulative correlation coefficient (CCC), i.e., the maximum of the stacked similarity matrix. The dv/v estimated from the two-day smoothed similarity matrices are plotted in black. The blue curve indicates hourly precipitation in water equivalent. Grey bars correspond to the snow-depth in water equivalent. Vertical red-dashed lines are the origin times of local earthquakes with magnitudes>4.8.

Results

Following events of precipitation, we find two types of responses: (1) A short term velocity decrease and (2) a long term velocity increase, which we deem to be a result of pore-space compaction due to the increasing snow load.

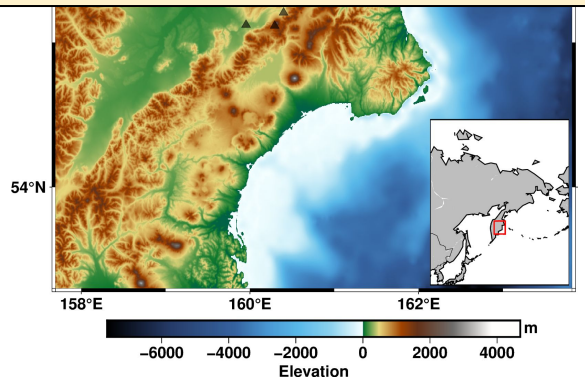

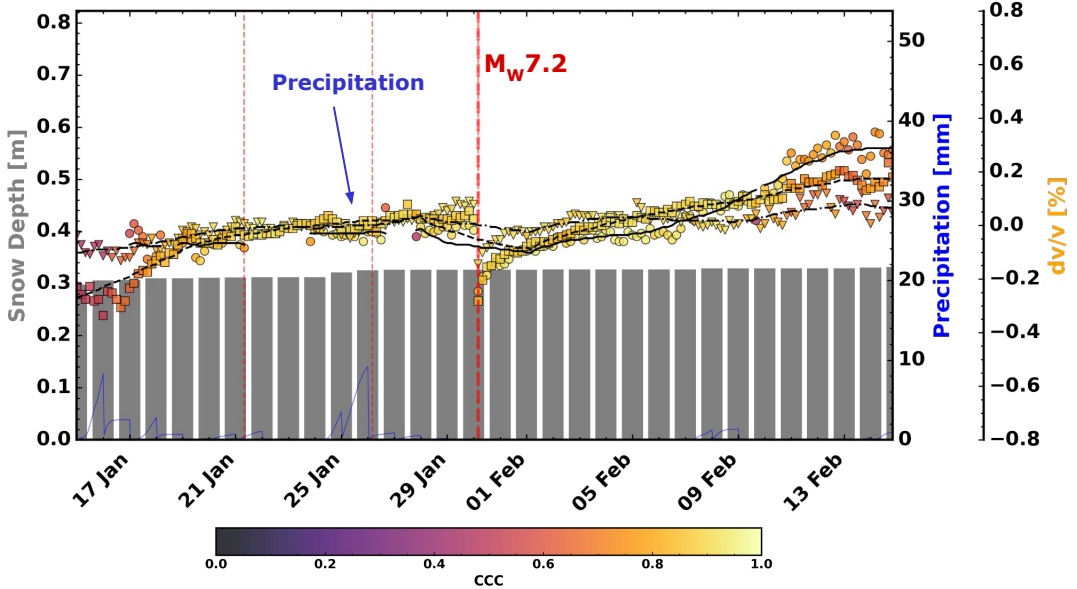

Fig: (Left) A map view of the study area. The location of Bezymianny volcano is depicted.Grey stations are failing or out-of-order during the targeted times. Stations shown in black are available though not discussed. Orange stations are used for the "triangle" and the "square group". (Right) dv/v time series for coloured groups of stations on the map (symbols are identical). Each point corresponds to the dv/v of a two-hours time window. The points' colour scale with the cumulative correlation coefficient (CCC), i.e., the maximum of the stacked similarity matrix. The dv/v estimated from two-day smoothed similarity matrices are plotted in black. The blue curve indicates hourly precipitation in water equivalent. Grey bars correspond to the snow-depth in water equivalent. Vertical red-dashed lines are origin times of local earthquakes with magnitudes>4.8.

Results

Lastly, we see a velocity increase in early February at stations in the proximity of Bezymianny volcano, in particular at D0.BZG (circles). This increase may be related to a beginning inflation at Bezymianny reported by Mania et, al. (2019).

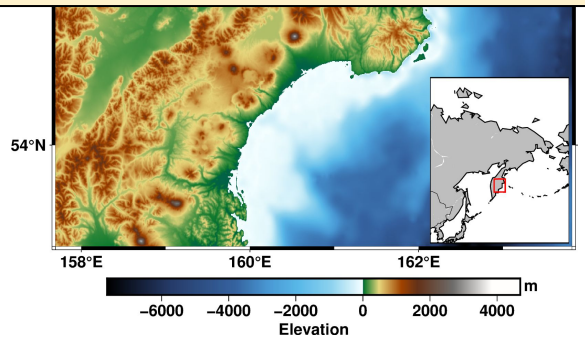

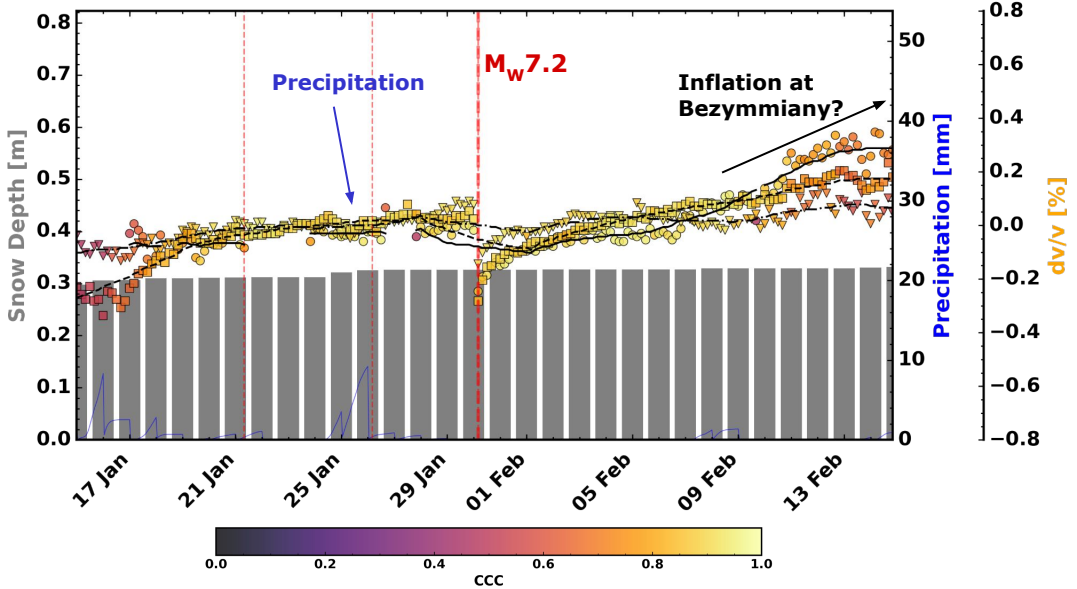

Fig: (Left) A map view of the study area. The location of Bezymianny volcano is depicted.Grey stations are failing or out-of-order during the targeted times. Stations shown in black are available though not discussed. Orange stations are used for the "triangle" and the "square" group. (Right) dv/v time series for coloured groups of stations on the map (symbols are identical). Each point corresponds to the dv/v of a two-hours time window. The points' colour scales with the cumulative correlation coefficient (CCC), i.e., the maximum of the stacked similarity matrix. The dv/v estimated from the two-day smoothed similarity matrices are plotted in black. The blue curve indicates hourly precipitation in water equivalent. Grey bars correspond to the snow-depth in water equivalent. Vertical red-dashed lines are the origin times of local earthquakes with magnitudes>4.8.

Results

In spring and early summer, we can see a strong velocity decrease that we attribute to the inset of thawing (i.e., decreasing snow load, increasing water content). Even a reaction to a temporary stagnation in snow depth in early June has a clear impact on the evolution of dv/v.

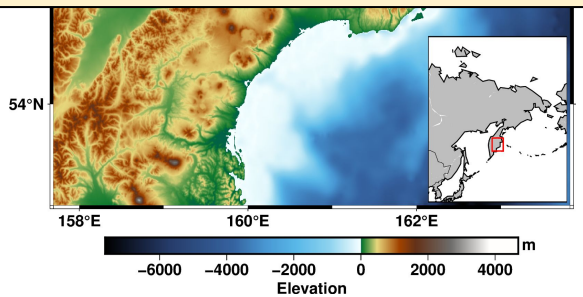

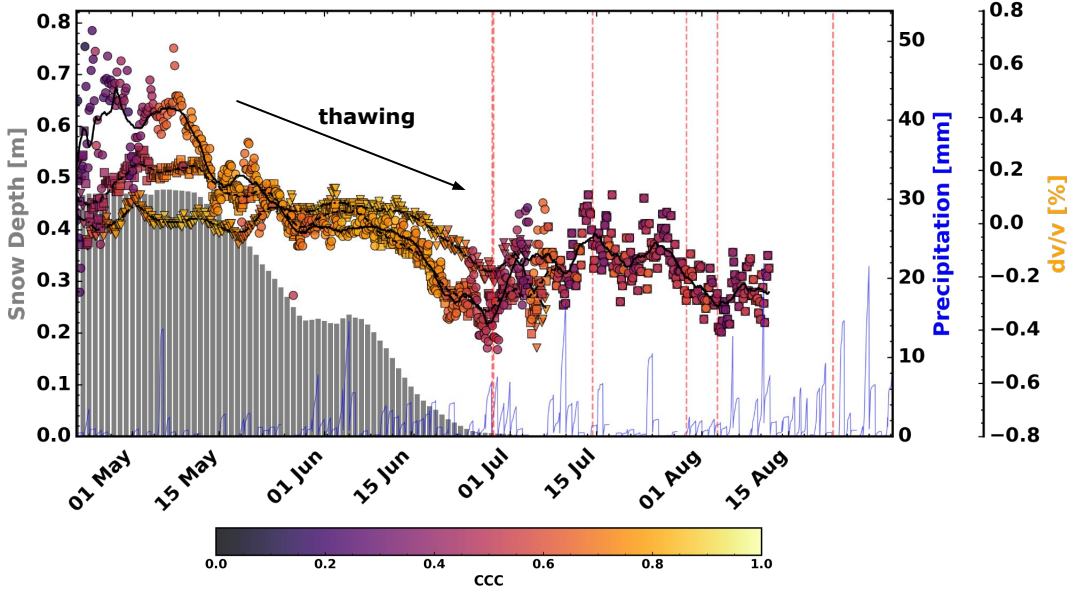

Fig: (Left) A map view of the study area. The location of Bezymianny volcano is depicted.Grey stations are failing or out-of-order during the targeted times. Stations shown in black are available though not discussed. Orange stations are used for the "triangle" and the "square group". (Right) dv/v time series for coloured groups of stations on the map (symbols are identical). Each point corresponds to the dv/v of a two-hours time window. The points' colour scale with the cumulative correlation coefficient (CCC), i.e., the maximum of the stacked similarity matrix. The dv/v estimated from two-day smoothed similarity matrices are plotted in black. The blue curve indicates hourly precipitation in water equivalent. Grey bars correspond to the snow-depth in water equivalent. Vertical red-dashed lines are origin times of local earthquakes with magnitudes>4.8.

Conclusions & Outlook

- A combination of spatial stacking and carefully selecting periods of high-energy volcanic tremors allows us to extract stable, highly-resolving velocity time series from an unstable noise field.
- We recover dv/v responses to seismic and environmental events. The responses vary significantly with the geological and geographical setting of the stations.
- In February 2016, we observe potential indicators for an inflation at Bezymianny volcano.
- For future work, we expect to unravel smaller contributions by removing the response to meteorological factors by subtracting an appropriate model.

References

Baron, D., & Ménard, B. (2021). Extracting the Main Trend in a Data Set: The Sequencer Algorithm. *The Astrophysical Journal*, *916*(2), 91.

De Plaen, R. S., Lecocq, T., Caudron, C., Ferrazzini, V., & Francis, O. (2016). Single-station monitoring of volcanoes using seismic ambient noise. *Geophysical Research Letters*, *43*(16), 8511-8518.

Donaldson, C., Caudron, C., Green, R. G., Thelen, W. A., & White, R. S. (2017). Relative seismic velocity variations correlate with deformation at Kīlauea volcano. *Science advances*, *3*(6), e1700219.

Hirose, T., Nakahara, H., & Nishimura, T. (2017). Combined use of repeated active shots and ambient noise to detect temporal changes in seismic velocity: Application to Sakurajima volcano, Japan. *Earth, Planets and Space*, *69*(1), 1-12.

Journeau, C., Shapiro, N. M., Seydoux, L., Soubestre, J., Koulakov, I. Y., Jakovlev, A. V., ... & Jaupart, C. (2022). Seismic tremor reveals active trans-crustal magmatic system beneath Kamchatka volcanoes. *Science advances*, *8*(5), eabj1571.

Lesage, P., Reyes-Dávila, G., & Arámbula-Mendoza, R. (2014). Large tectonic earthquakes induce sharp temporary decreases in seismic velocity in Volcán de Colima, Mexico. *Journal of Geophysical Research: Solid Earth*, *119*(5), 4360-4376.

Machacca-Puma, R., Lesage, P., Larose, E., Lacroix, P., & Anccasi-Figueroa, R. M. (2019). Detection of pre-eruptive seismic velocity variations at an andesitic volcano using ambient noise correlation on 3-component stations: Ubinas volcano, Peru, 2014. *Journal of Volcanology and Geothermal Research*, *381*, 83-100.

Mania, R., Walter, T. R., Belousova, M., Belousov, A., & Senyukov, S. L. (2019). Deformations and morphology changes associated with the 2016–2017 eruption sequence at Bezymianny Volcano, Kamchatka. *Remote Sensing*, *11*(11), 1278.

Nakata, N., Gualtieri, L., & Fichtner, A. (Eds.). (2019). *Seismic ambient noise*. Cambridge University Press.

Sens-Schönfelder, C., & Wegler, U. (2006). Passive image interferometry and seasonal variations of seismic velocities at Merapi Volcano, Indonesia. *Geophysical research letters*, *33*(21).

Obermann, A., Planès, T., Larose, E., & Campillo, M. (2013). Imaging preeruptive and coeruptive structural and mechanical changes of a volcano with ambient seismic noise. *Journal of Geophysical Research: Solid Earth*, *118*(12), 6285-6294.

Shapiro, N. M., Sens-Schönfelder, C., Lühr, B., Weber, M., Abkadyrow, I., Gordeev, E. I., ... & Saltykov, V. A. (2017). Understanding Kamchatka's extraordinary volcano cluster. *Eos, Transactions American Geophysical Union*, (98).

Volcano Symbol: Volcano by Brand Mania from NounProject.com